



ELSEVIER

Available online at [www.sciencedirect.com](http://www.sciencedirect.com)

SCIENCE @ DIRECT®

Journal of Sound and Vibration 289 (2006) 967–986

JOURNAL OF  
SOUND AND  
VIBRATION

[www.elsevier.com/locate/jsvi](http://www.elsevier.com/locate/jsvi)

# On maximal eigenfrequency separation in two-material structures: the 1D and 2D scalar cases

Jakob S. Jensen<sup>a,\*</sup>, Niels L. Pedersen<sup>b</sup>

<sup>a</sup>*Department of Mechanical Engineering, Technical University of Denmark, Nils Koppels Allé,  
Building 404, DK-2800 Kgs. Lyngby, Denmark*

<sup>b</sup>*Institute of Mechanical Engineering, Aalborg University, Pontoppidanstræde 101, DK-9220 Aalborg East, Denmark*

Received 1 March 2004; received in revised form 7 February 2005; accepted 1 March 2005

Available online 8 August 2005

---

## Abstract

We present a method to maximize the separation of two adjacent eigenfrequencies in structures with two material components. The method is based on finite element analysis and topology optimization in which an iterative algorithm is used to find the optimal distribution of the materials. Results are presented for eigenvalue problems based on the 1D and 2D scalar wave equations. Two different objectives are used in the optimization, the difference between two adjacent eigenfrequencies and the ratio between the squared eigenfrequencies. In the 1D case, we use simple interpolation of material parameters but in the 2D case the use of a more involved interpolation is needed, and results obtained with a new interpolation function are shown. In the 2D case, the objective is reformulated into a double-bound formulation due to the complication from multiple eigenfrequencies. It is shown that some general conclusions can be drawn that relate the material parameters to the obtainable objective values and the optimized designs.

© 2005 Elsevier Ltd. All rights reserved.

---

## 1. Introduction

One strategy for the passive vibration control of mechanical structures is to design the structures so that eigenfrequencies lie as far away as possible from the excitation frequencies. This paper exploits the possibility for using the method of topology optimization to maximize the

---

\*Corresponding author. Tel.: +45 45 25 4280; fax: +45 45 93 1475.

E-mail address: [jsj@mek.dtu.dk](mailto:jsj@mek.dtu.dk) (J.S. Jensen).

separation of two adjacent eigenfrequencies in structures with two material components. This study is restricted to 1D and 2D structures where the vibrations are governed by the scalar wave equation.

The method of topology optimization [1] has been used to optimize a number of different mechanical and physical systems [2]. The original formulation using a homogenization approach was applied by Diaz and Kikuchi [3] for eigenfrequency optimization. The problem was formulated as a reinforcement problem in which a given structure is reinforced in order to maximize eigenfrequencies. Soto and Diaz [4] considered optimal design of plate structures and they maximized higher-order eigenfrequencies and also two eigenfrequencies simultaneously. Ma et al. [5] used the same formulation to maximize the sums of a number of the lowest eigenfrequencies and also considered maximization of gaps between eigenfrequencies of low-order modes for structures with concentrated masses. Topology optimization using interpolation schemes (e.g. SIMP with penalization) or similar material interpolation models [6], was used by Kosaka and Swan [7] to optimize the sum of low-order eigenfrequencies. In Ref. [8] topology optimization was used to maximize eigenfrequencies of plates. Here, the problem was not formulated as a reinforcement problem and emphasis was laid on the use of an interpolation function different from SIMP. Recently, optimization of the lowest eigenfrequencies for plates subjected to pre-stress has been considered [9].

The separation of adjacent eigenfrequencies is closely related to the existence of gaps in the band structure characterizing wave propagation in periodic elastic materials [10], often referred to as phononic band gaps. This is illustrated by the 1D example in Fig. 1, showing an elastic rod subjected to time-harmonic longitudinal excitation. The rod is made from a periodic material with two components PMMA and aluminum. It can be shown that there are large gaps in the band structure corresponding to frequency ranges where longitudinal waves cannot propagate through the compound material. The implication for the corresponding structure is that no eigenfrequencies exist in these band gap frequency ranges, except possibly for localized modes

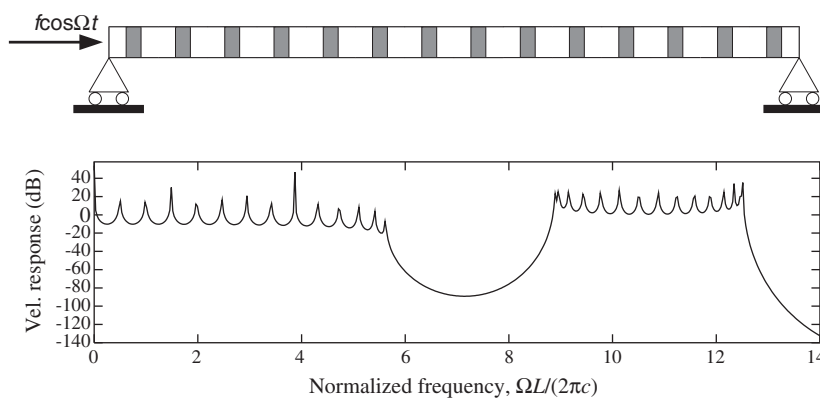


Fig. 1. Longitudinal vibrations of a PMMA rod with 14 periodically placed aluminum inclusions subjected to time-harmonic excitation at the left end. The bottom figure shows the velocity response at the right end versus the normalized excitation frequency  $\Omega L/(2\pi c)$ , where  $L$  is the rod length and  $c$  is the wave speed in PMMA. Material properties are  $\rho_{\text{PMMA}} = 1200 \text{ kg/m}^3$ ,  $\rho_{\text{alu}} = 2700 \text{ kg/m}^3$ ,  $E_{\text{PMMA}} = 5.3 \text{ GPa}$  and  $E_{\text{alu}} = 70 \text{ GPa}$ .

near the boundaries [11]. The resulting gaps between two adjacent eigenfrequencies may be large, as seen from the frequency response curve in the figure, and the corresponding response in the gaps when subjected to time-harmonic excitation may be very low.

Topology optimization and related methods have previously been applied to maximize the band gaps in periodic materials for photonic band gaps, i.e. for electromagnetic waves [12,13] and by Sigmund [14] for phononic band gaps. Minimizing the response for band gap structures, i.e. creating a structure with a response as low as possible (cf. Fig. 1), was considered by Sigmund and Jensen [15]. Other works have considered minimizing the vibrational response of structures, such as Ma et al. [16] who used the homogenization approach for the optimal design of structures with low response and in Ref. [17] where structures subjected to time-harmonic loading were optimized with respect to dynamic compliance.

Osher and Santosa [18] used a level set method to study extremal eigenvalue problems for a two-material drum, considering also the case of maximizing the gap between the first and second eigenfrequencies. The present paper extends these results by considering the more general scalar wave equation problem and by systematically considering separation of eigenfrequencies of arbitrary order. We start by treating the simplest problem of structures for which the vibrations are governed by the 1D wave equation and present results for maximizing the gap between two eigenfrequencies and also for an alternative formulation that considers the ratio of adjacent eigenfrequencies. Then we consider the more complicated problem of 2D structures and show results for both optimization formulations. In the 2D case we introduce a new interpolation of the material parameters in order to ensure a final 0–1 design, i.e. a design with a clear separation of the use of the two materials. Additionally, we must treat multiple eigenfrequencies which are present in the optimized designs. The treatment of multiple eigenfrequencies is primarily related to the sensitivity calculation but we also reformulate the objective of the optimization into a double-bound formulation which gives stable convergence. Finally, we present some conclusions.

## 2. The 1D scalar problem

First, we treat the simplest problem of separating eigenfrequencies for the 1D scalar problem.

### 2.1. Model

Consider the 1D scalar time-reduced wave equation (Helmholtz equation):

$$(A(x)w')' + \omega^2 B(x)w = 0, \quad (1)$$

subjected to free–free boundary conditions at  $x = 0$  and  $x = L$ .

Eq. (1) governs eigenvibrations of different mechanical systems depending on the choice of the coefficients  $A$  and  $B$ . For  $A = 1$  and  $B = \tilde{\rho}/T$  we can interpret the problem as that of transverse vibrations of a taut string with  $\tilde{\rho}(x)$  and  $T$  being the string mass per length and the tensile force, respectively. For  $A = E$  and  $B = \rho$  we instead treat the problem of longitudinal vibrations of a uniform rod. In this case,  $E(x)$  is Young's modulus and  $\rho(x)$  is the density. Similarly, with another set of coefficients we can treat the problem of torsional vibrations of a rod.

To solve the wave equation with in-homogeneous coefficients we apply a standard Galerkin finite element discretization of Eq. (1) and the boundary conditions, which lead to the discrete eigenvalue problem:

$$\mathbf{K}\boldsymbol{\phi} = \omega^2\mathbf{M}\boldsymbol{\phi}, \quad (2)$$

which has  $(\omega_i, \boldsymbol{\phi}_i)$  as the  $i$ th eigensolution (frequency and vector), and where  $\mathbf{M}$  and  $\mathbf{K}$  are system matrices given by

$$\mathbf{K} = \sum_{e=1}^N A_e \mathbf{k}_e, \quad \mathbf{M} = \sum_{e=1}^N B_e \mathbf{m}_e, \quad (3)$$

where the summations should be understood in the normal finite element sense, and  $\mathbf{k}_e$  and  $\mathbf{m}_e$  are element matrices defined as

$$\mathbf{k}_e = \int_{V_e} \frac{d\mathbf{N}^T}{dx} \frac{d\mathbf{N}}{dx} dV, \quad \mathbf{m}_e = \int_{V_e} \mathbf{N}^T \mathbf{N} dV, \quad (4)$$

where  $\mathbf{N}$  is the shape function vector for the chosen element type. In this work, we use simple elements, i.e. a 2-node linear element for the 1D case and later a 4-node bilinear quadratic element for the 2D case.

This finite element formulation for the problem is now the basis for the optimization procedure presented in the following.

## 2.2. Optimization

The basis of topology optimization with a material interpolation scheme is to assign constant material properties to each element in the finite element model and then associate these material properties with continuous design variables [2]. We choose one design variable per element and let it vary continuously between 0 and 1:

$$t_e \in \mathbb{R} \mid 0 \leq t_e \leq 1, \quad e \in [1, N], \quad (5)$$

where  $N$  is the number of finite elements in the model.

We now let the material properties in each element,  $A_e$  and  $B_e$ , be a specified interpolation function of this design variable. This is done so that the material properties for  $t_e = 0$  correspond to material 1, i.e.  $A_1$  and  $B_1$ , and similarly for  $t_e = 1$  they take the values of material 2,  $A_2$  and  $B_2$ . We emphasize the fundamental difference between this approach in which we use a continuous design variable that allows us to apply well-founded gradient-based optimization techniques, and the use of discrete design variables that requires integer-type algorithms.

Since  $t_e$  vary continuously between 0 and 1 we may expect that in the optimal design we can end up with material properties that do not correspond to either of the two materials, but instead with some intermediate values. In order to ensure a well-defined distribution of materials 1 and 2 in the structure, referred to as a 0–1 design, we can manipulate the interpolation functions [6]. Especially when dealing with eigenvalue problems the choice of the interpolation function is important [8]. However, for the 1D problem the choice is less critical and we choose the functions:

$$A_e(t_e) = A_1 + t_e(A_2 - A_1) = (1 + t_e(\mu_A - 1))A_1, \quad (6)$$

$$B_e(t_e) = \frac{B_1}{1 + t_e \left( \frac{B_1}{B_2} - 1 \right)} = \frac{B_1}{1 + t_e (\mu_B^{-1} - 1)}, \tag{7}$$

which correspond to the homogenized density ( $B_e$ ) and stiffness ( $A_e$ ) of an “effective” 1D material with two different material components. As will appear later this is sufficient to ensure the wanted 0–1 design. In Eqs. (6)–(7) the coefficient contrast parameters  $\mu_A = A_2/A_1$  and  $\mu_B = B_2/B_1$  have been introduced.

We now define the difference between two adjacent eigenfrequencies  $\omega_n$  and  $\omega_{n+1}$  as our objective for the optimization to maximize. This can be written as a standard optimization problem as follows:

$$\begin{aligned} \max_{t_e} \quad & J = \omega_{n+1} - \omega_n \\ \text{s.t.} \quad & \mathbf{K}\boldsymbol{\phi} = \omega^2 \mathbf{M}\boldsymbol{\phi} \\ & 0 \leq t_e \leq 1, \quad e \in [1, N]. \end{aligned} \tag{8}$$

The maximization problem in Eq. (8) is solved using an iterative procedure involving the following steps:

1. Choose  $n$  for the optimization problem.
2. Choose an initial design  $t_e$ , typically chosen as a homogeneous material distribution (e.g.  $t_e = 0.5$  for all elements).
3. Calculate the  $M$  lowest eigenfrequencies ( $M > n + 1$ ) from Eq. (2) and compute the objective function  $J$ .
4. Calculate the sensitivities  $dJ/dt_e$ .
5. Get a design update using an optimizing routine, e.g. MMA [19].
6. Repeat steps 3–5 until the design change between successive iterations is less than a specified tolerance.

The sensitivity of the objective function is calculated analytically

$$\frac{dJ}{dt_e} = \frac{d\omega_{n+1}}{dt_e} - \frac{d\omega_n}{dt_e}, \tag{9}$$

where the sensitivity of the  $n$ th eigenvalue is

$$\frac{d\omega_n}{dt_e} = \frac{\frac{dA_e}{dt_e} u_{\text{ela}} - \omega_n^2 \frac{dB_e}{dt_e} u_{\text{kin}}}{2\omega_n}, \tag{10}$$

where we assume that only  $A_e$  and  $B_e$  are functions of the design variable  $t_e$  on an element level. It is also assumed that the eigenvectors have been normalized so that  $\boldsymbol{\phi}^T \mathbf{M}\boldsymbol{\phi} = 1$ , and that

$$u_{\text{kin}} = (\boldsymbol{\phi}_e)_n^T \mathbf{m}_e(\boldsymbol{\phi}_e)_n, \tag{11}$$

$$u_{\text{ela}} = (\boldsymbol{\phi}_e)_n^T \mathbf{k}_e(\boldsymbol{\phi}_e)_n, \tag{12}$$

are the element-specific kinetic and elastic energies for the given mode of order  $n$ .

In the following section, we show results for a specific choice of the material coefficients. We consider free–free boundary conditions and enumerate the rigid body mode as  $n = 0$ .

### 2.3. Results—the elastic rod

In the example, we use the values  $\mu_A = 13.21$  and  $\mu_B = 2.25$ . This corresponds to the ‘elastic rod’ problem of longitudinal vibrations with PMMA and aluminum as the two materials to be distributed. The objective of the optimization is to distribute the two materials in such a way that the eigenfrequency gap  $\omega_{n+1} - \omega_n$  is maximized.

Results are shown in Fig. 2 for maximizing the gap for four different cases:  $n = 1$ ,  $n = 2$ ,  $n = 9$ , and  $n = 24$ . The figures on the left show the material distribution in the optimized designs with the relative element position indicated along the abscissa. The figures on the right are the results of subjecting the optimized structure to time-harmonic excitation at the left end and computing the velocity response at the right end. The curves show the response versus the normalized excitation frequency  $\Omega L/(2\pi c)$ , where  $L$  is the rod length and  $c = \sqrt{A_1/B_1}$  is the wave speed in material 1. From these curves the discrete eigenfrequencies of the structure are easily identified by the peaks.

The most important result is that the designs consist of alternating sections of  $t_e = 0$  (material 1) and  $t_e = 1$  (material 2); thus the structures are well defined in terms of distribution of materials 1 and 2. Furthermore, there is a direct relation between the mode order  $n$  and the number of sections with material 2 (inclusions) that appear. The inclusions also appear to have a uniform size in the interior of the structure, and only near the rod ends the effect of the boundary conditions may be seen as a local modification of the material distribution. For high-order mode separation ( $n = 9$  and  $24$ ) the optimized gap between mode  $n$  and  $n + 1$  becomes significantly larger than the gaps between other adjacent modes, and a low-velocity response is noted in the maximized gap. For low-order modes ( $n = 1$  and  $2$ ) the difference in gaps is smaller and the response drop in the maximized gap is hardly distinguishable compared to the drop in response between the other eigenfrequencies.

### 2.4. Maximizing the ratio of adjacent eigenfrequencies

Instead of maximizing the gap between two adjacent eigenfrequencies we now maximize the ratio between the two eigenfrequencies (or rather the square of the frequencies). The new objective function is

$$J = \frac{\omega_{n+1}^2}{\omega_n^2}, \quad (13)$$

and the corresponding expression for the sensitivities is given as

$$\frac{dJ}{dt_e} = 2 \frac{\omega_{n+1}}{\omega_n^2} \left( \frac{d\omega_{n+1}}{dt_e} - \frac{\omega_{n+1}}{\omega_n} \frac{d\omega_n}{dt_e} \right), \quad (14)$$

where  $d\omega_n/dt_e$  and  $d\omega_{n+1}/dt_e$  are found from Eq. (10).

In order to compare the designs obtained using this new objective function with the previous, results are shown with  $\mu_A$  and  $\mu_B$  as in Section 2.3 for two different modes,  $n = 4$  and  $n = 19$ . The

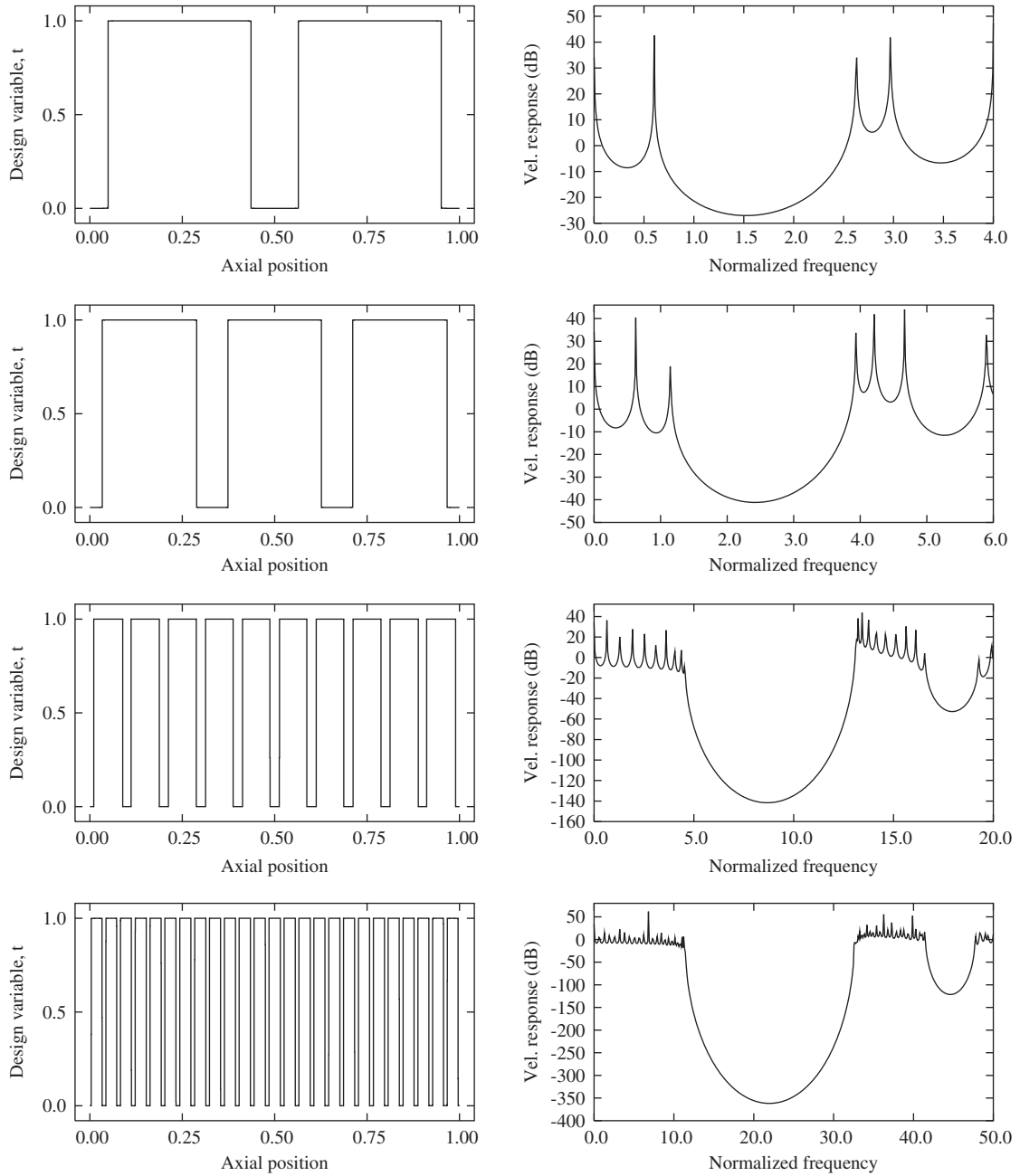


Fig. 2. Optimized design (left) and corresponding velocity response (right) for maximum separation of  $\omega_{n+1}$  and  $\omega_n$ . The material parameters correspond to the ‘elastic rod case’ with  $\mu_A = 13.21$ ,  $\mu_B = 2.25$ . Results are given for four different values of  $n$ , from top to bottom:  $n = 1, 2, 9, 24$ .

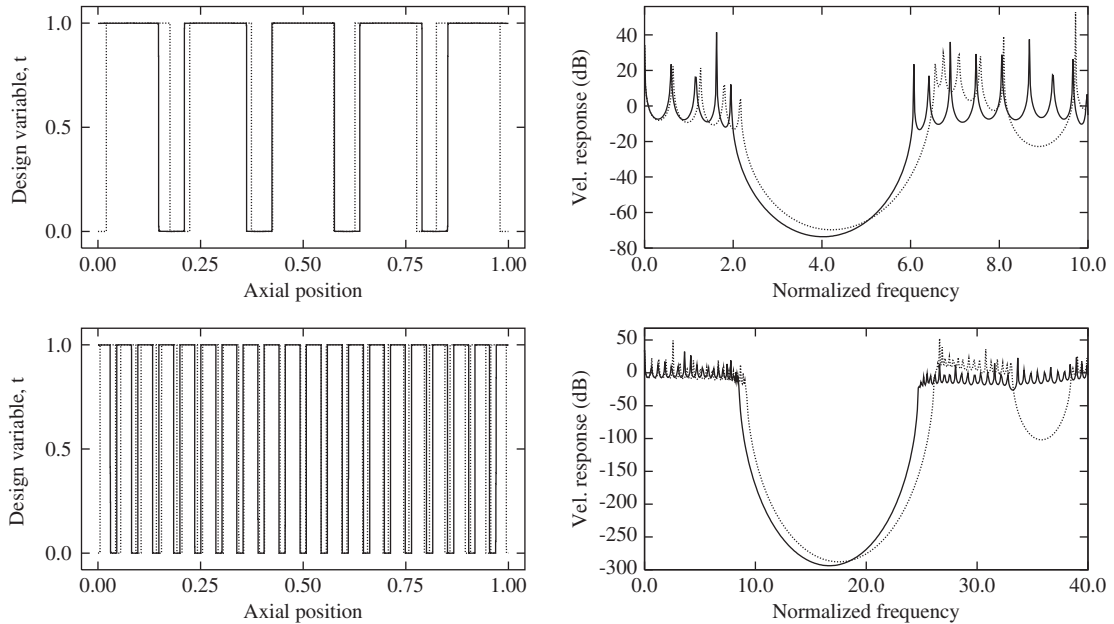


Fig. 3. Comparison of optimized design (left) and velocity response (right) for maximizing the eigenfrequency gap  $\omega_{n+1} - \omega_n$  (dotted lines) and maximizing the eigenfrequency ratio  $\omega_{n+1}^2/\omega_n^2$  (solid lines). Material parameters are as for Fig. 2 and results are given for  $n = 4$  and 19.

comparison is shown in Fig. 3 with the results for the new objective function plotted with solid lines and for the old objective function with dotted lines.

The material distribution curves left show that the new objective function has caused a shift in the distribution between materials 1 and 2 and that the material in the end of the rods is now material 2 instead of material 1. Interestingly, the response curves on the right show that the response in the gaps optimized for maximum ratio drops lower in both examples even though the absolute gap size is smaller for these designs.

We now introduce a material parameter  $\beta$  that characterizes the contrast between materials

$$\beta = \mu_A \mu_B > 1, \tag{15}$$

where the last inequality condition just implies that if not fulfilled the enumeration of the two materials should be interchanged.

In Fig. 4, we show results for maximizing the ratio of eigenfrequencies for three different combinations of material coefficients but keeping  $\beta = 4$ . We vary  $\mu_A$  and  $\mu_B$  such that in the top figures  $\mu_A = \mu_B$ , in the middle figures  $\mu_A = 4, \mu_B = 1$ , and in the bottom figures  $\mu_A = 1$  and  $\mu_B = 4$ . For all three combinations we maximize the ratio for  $n = 4$  and find that the ratio for the optimized designs in all cases becomes 3.09. For other combinations of material coefficients and when optimizing for other  $n$ , we see that the maximum ratio between the adjacent eigenfrequencies obtainable for any mode order seems to depend only on the parameter  $\beta$ . However, as also seen in the figure, the material distribution varies and there is also a large difference in the response curves for the different combinations of material coefficients.



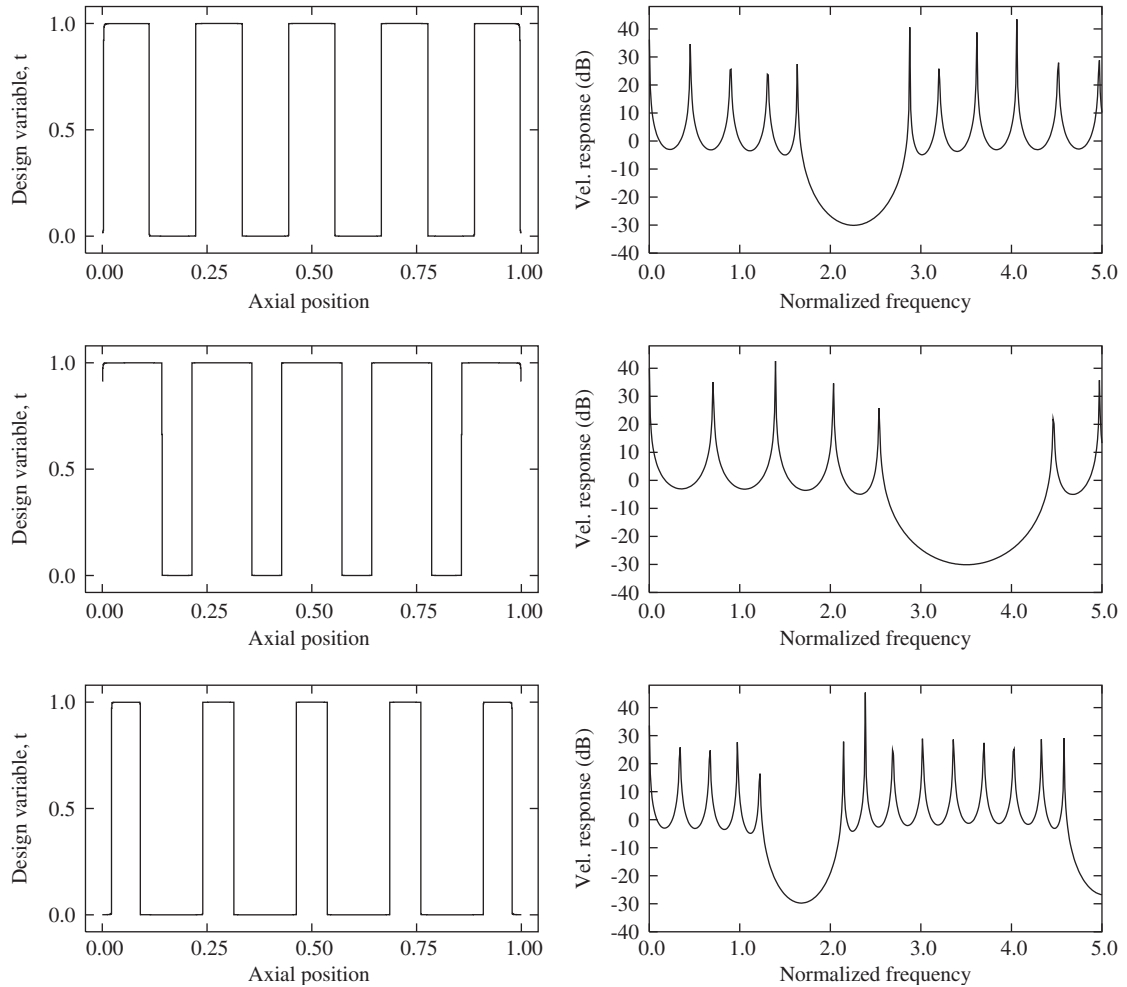


Fig. 4. Optimized design (left) and corresponding velocity response (right) for maximized eigenvalue ratio  $\omega_5^2/\omega_4^2$  for three different choices of  $\mu_A$  and  $\mu_B$ , top:  $\mu_A = \mu_B = 2$ , middle:  $\mu_A = 4$ ,  $\mu_B = 1$ , and bottom:  $\mu_A = 1$ ,  $\mu_B = 4$ . The maximum ratio is (for  $n = 4$  as shown) for all three cases equal to 3.09.

We now plot the maximum obtainable eigenfrequency ratio versus mode order  $n$  for different values of the parameter  $\beta$ . Fig. 5 shows the maximum ratio for three different values of  $\beta$ , corresponding to the combination of coefficients for the elastic rod ( $\beta \approx 29.7$ ), as well as for  $\beta = 2$  and  $\beta = 9$ . The ratio for a homogeneous structure which is given by the analytical expression  $\omega_{n+1}^2/\omega_n^2 = (n + 1)^2/n^2$  is also shown in the figure. Naturally, for higher contrast, i.e. higher values of  $\beta$ , the maximum ratio is higher. Also it appears that for high values of  $n$  this ratio attains a constant value.

Fig. 4 shows that although the eigenfrequency ratio for the optimal design depends only on the value of the parameter  $\beta$ , the material distribution depends on the chosen values of the material

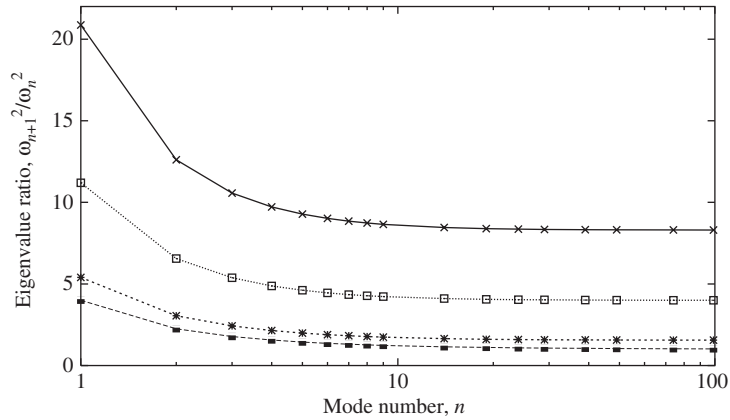


Fig. 5. The maximum eigenfrequency ratio  $\omega_{n+1}^2/\omega_n^2$  as a function of the mode order  $n$ . Curves are presented for the homogeneous case (■) as well as for three values of  $\beta = \mu_A\mu_B$ :  $\beta = 2$  (\*),  $\beta = 9$  (□), and  $\beta = 29.7$  (×), the latter corresponding to the elastic rod case.

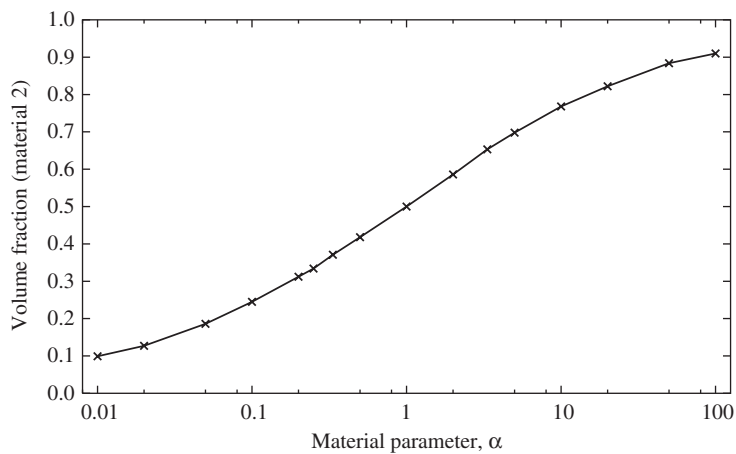


Fig. 6. Fraction of material 2 in the optimized design as a function of the material parameter  $\alpha = \mu_A/\mu_B$ . The fraction is calculated in the middle of the structure where the end effects do not play a role.

coefficients. In order to analyze this effect, a second material parameter is introduced:

$$\alpha = \frac{\mu_A}{\mu_B}. \tag{16}$$

We now optimize the ratio for different material coefficients but keep  $\alpha$  constant. In this case the optimized material distribution is always the same, whereas the maximum eigenvalue ratio varies significantly. In Fig. 6, we plot the volume fraction of material 2 versus the value of  $\alpha$ . The volume fraction is computed in the interior part of the domain where the boundary effects are not important. As seen, with  $\alpha = 1$  the two materials are evenly distributed in the optimized design,

whereas if  $\alpha$  is increased material 2 is dominating and for lower values of  $\alpha$  material 1 is dominating. If  $\mu_A = 1$  (e.g. a taut string) we have  $\alpha = 1/\beta < 1$  which shows that material 1 (the lighter material) is always dominant in the optimized design for this special case.

### 3. The 2D scalar case

We now consider the more complex problem of the 2D scalar case.

#### 3.1. Model

The 2D scalar time-reduced wave equation (Helmholtz equation) is given by

$$\nabla^T(A(x,y)\nabla w) + \omega^2 B(x,y)w = 0, \tag{17}$$

where the problem-dependent material coefficients  $A$  and  $B$  can now vary in the 2D plane  $(x,y)$ . As in the 1D case we apply a standard FEM discretization, which leads to the discrete eigenvalue problem stated in Eqs. (2)–(3). The element matrices are in the 2D case given by

$$\mathbf{k}_e = \int_{V_e} (\mathbf{\partial N})^T \mathbf{\partial N} dV, \quad \mathbf{m}_e = \int_{V_e} \mathbf{N}^T \mathbf{N} dV, \tag{18}$$

where

$$\mathbf{\partial} = \begin{bmatrix} \partial/\partial x & 0 \\ 0 & \partial/\partial y \end{bmatrix}. \tag{19}$$

Also in the 2D case we may study different structural vibration problems by changing the two coefficients  $A$  and  $B$ . Letting  $A = 1$  and  $B = \rho/T$  enables us to analyze the membrane problem where  $\rho(x,y)$  is the density and  $T$  is the uniform tension (force per area). Alternatively with  $A = E/(2(1 + \nu))$ , where  $E(x,y)$  is Young’s modulus and  $\nu(x,y)$  is Poisson’s ratio, and with  $B = \rho(x,y)$  being the density, Eq. (19) governs out-of-plane shear vibrations of a thick elastic body.

#### 3.2. Optimization

When we optimize a 2D domain with respect to maximizing the gap between eigenfrequencies there are a number of extra difficulties we must deal with. The primary source of the difficulties is the possibility of multiple eigenfrequencies. The multiple eigenfrequencies can be calculated without difficulty using, e.g. the subspace iteration method [20].

The objective for the optimization is as in the 1D case given by

$$\text{maximize } J = \omega_{n+1} - \omega_n, \tag{20}$$

where the gap between the eigenfrequency of order  $n + 1$  and  $n$  is maximized.

If the eigenfrequencies of order  $n + 1$  and  $n$  are both distinct eigenpairs, with squared eigenfrequencies  $\omega_{n+1}^2$  and  $\omega_n^2$  and corresponding eigenvectors  $\phi_{n+1}$  and  $\phi_n$ , no problems arise and we use the objective (20) directly since the sensitivities of the squared eigenfrequency with respect

to a design parameter  $t_e$  are given by

$$\frac{d\omega^2}{dt_e} = \boldsymbol{\Phi}^T \left( \frac{d\mathbf{K}}{dt_e} - \omega^2 \frac{d\mathbf{M}}{dt_e} \right) \boldsymbol{\Phi}, \tag{21}$$

where it is assumed that the eigenvector has been normalized so that  $\boldsymbol{\Phi}^T \mathbf{M} \boldsymbol{\Phi} = 1$ . In the case of multiple eigenvalues we cannot use Eq. (21) to find the sensitivities. The extended method is presented in Ref. [21] and was used more recently in Ref. [22].

We elaborate on the case of a double eigenfrequency with two corresponding eigenvectors,  $(\omega^2, \boldsymbol{\Phi}_1, \boldsymbol{\Phi}_2)$ . It is assumed that the two eigenvectors are normalized with respect to the mass matrix as before and that the two eigenvectors are orthogonal, i.e.,

$$\boldsymbol{\Phi}_1^T \mathbf{M} \boldsymbol{\Phi}_2 = 0. \tag{22}$$

The problem is that any linear combination of the two eigenvectors is also an eigenvector with the same corresponding eigenfrequency:

$$\bar{\boldsymbol{\Phi}} = c_1 \boldsymbol{\Phi}_1 + c_2 \boldsymbol{\Phi}_2, \tag{23}$$

$$c_1^2 + c_2^2 = 1 \Rightarrow \bar{\boldsymbol{\Phi}}^T \mathbf{M} \bar{\boldsymbol{\Phi}} = 1. \tag{24}$$

Therefore, the sensitivities are not only related to the change in design space, given by the change in design parameter  $t_e$ , but also by the choice of the eigenvector. Only for two specific eigenvectors, depending on the design parameter, do the sensitivities have meaning, because only these two eigenvectors exist when  $t_e$  is changed. By inserting Eq. (23) in Eq. (21) we get

$$\frac{d\omega^2}{dt_e} = c_1^2 g_{11} + c_2^2 g_{22} + 2c_1 c_2 g_{12}, \tag{25}$$

$$g_{\alpha\beta} = \boldsymbol{\Phi}_\alpha^T \left( \frac{d\mathbf{K}}{dt_e} - \omega^2 \frac{d\mathbf{M}}{dt_e} \right) \boldsymbol{\Phi}_\beta. \tag{26}$$

The extreme values of  $d\omega^2/dt_e$  are found by differentiating Eq. (25) with respect to the two constants  $c_1$  and  $c_2$  and setting this equal to zero

$$\begin{bmatrix} g_{11} & g_{12} \\ g_{12} & g_{22} \end{bmatrix} \begin{Bmatrix} c_1 \\ c_2 \end{Bmatrix} = \begin{Bmatrix} 0 \\ 0 \end{Bmatrix}, \tag{27}$$

and we now find the eigenvalues and the eigenvectors of the matrix in Eq. (27):

$$\left( g_a, \mathbf{c}_a = \begin{Bmatrix} c_{a1} \\ c_{a2} \end{Bmatrix} \right), \quad \left( g_b, \mathbf{c}_b = \begin{Bmatrix} c_{b1} \\ c_{b2} \end{Bmatrix} \right). \tag{28}$$

The sensitivities of the double eigenfrequency with respect to the design parameter  $t_e$  are given directly by  $g_a$  and  $g_b$ . The corresponding eigenvectors are given by Eq. (23) where the constants  $c_1$  and  $c_2$  are the values of the eigenvector  $\mathbf{c}_a$  or  $\mathbf{c}_b$ :

$$\frac{d\omega^2}{dt_e} = \begin{cases} g_a & \text{with eigenvector } \boldsymbol{\Phi}_a = c_{a1} \boldsymbol{\Phi}_1 + c_{a2} \boldsymbol{\Phi}_2, \\ g_b & \text{with eigenvector } \boldsymbol{\Phi}_b = c_{b1} \boldsymbol{\Phi}_1 + c_{b2} \boldsymbol{\Phi}_2. \end{cases} \tag{29}$$

For different design parameters the eigenvectors  $\phi_a$  and  $\phi_b$  vary, i.e. the sensitivities in Eq. (29) are given for two specific directions in the space spanned by the two originally determined eigenvectors ( $\phi_1, \phi_2$ ). The derivation shown here is for a double eigenfrequency but the extension to a higher number of multiplicity is straightforward.

It is now possible to find the sensitivities of multiple eigenfrequencies. However, there is still a problem because the sensitivities are given for specific eigenvectors that vary for each design parameter. It is therefore difficult to solve the optimization problem as formulated in Eq. (20). As an alternative formulation we propose to use a double-bound formulation, as in Ref. [14]. The standard-bound formulation is used to reformulate a min–max problem; instead of minimizing the maximum value of a given quantity, a new variable is introduced which is minimized subject to the constraint that the value of the given quantity should be less than this variable. By using the double-bound formulation we do not need to identify the two eigenvectors corresponding to  $\omega_n$  and  $\omega_{n+1}$  in each iteration step of the optimization, which may change from iteration to iteration. This is an advantage when we have multiple eigenfrequencies. The optimization problem of maximizing the gap between two eigenfrequencies is thus reformulated as

$$\begin{aligned}
 \max_{t_e} \quad & J = C_1 - C_2 \\
 \text{s.t.} \quad & \omega_{n+i} \geq C_1 \quad i \in [1, n_u] \\
 & \omega_{n+1-j} \leq C_2 \quad j \in [1, n_l] \\
 & \mathbf{K}\phi = \omega^2 \mathbf{M}\phi \\
 & 0 \leq t_e \leq 1, \quad e \in [1, N],
 \end{aligned} \tag{30}$$

where the two extra variables introduced are  $C_1$  and  $C_2$ . The numbers  $n_u$  and  $n_l$  are chosen suitable in order to secure that all eigenfrequencies of order  $n + 1$  and higher are greater than  $C_1$  and all eigenfrequencies of order  $n$  and lower are less than  $C_2$ .

In the practical implementation in each iteration step of the optimization we need to check if there are multiple eigenfrequencies and in this case calculate the sensitivities according to Eq. (29). It is important to note here that the sensitivities found for multiple eigenfrequencies are found for different eigenvectors for each design parameter. If the eigenfrequency of order  $n$  is a double eigenfrequency, which vector of sensitivities should we assign to the eigenfrequency of order  $n$  and which one to the eigenfrequency of order  $n - 1$ ? For a specific design parameter it is natural to assign the lowest sensitivity (including the sign) to the lowest order eigenfrequency ( $n - 1$ ) and the highest sensitivity to the highest order eigenfrequency ( $n$ ). If we make the infinitesimal design change the actual values of the involved eigenfrequencies comply with the chosen allocation of the sensitivities.

### 3.3. Penalization

The simplest interpolation of the material coefficients  $A$  and  $B$  when using two materials is made using a linear approach:

$$A_e(t_e) = A_1 + t_e(A_2 - A_1) = (1 + t_e(\mu_A - 1))A_1, \tag{31}$$

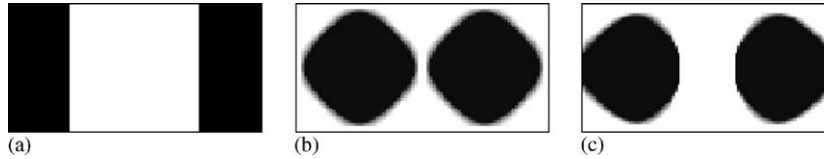


Fig. 7. Eigenfrequency optimization of a 2D domain with two different materials, the ratio of the side length is 2/1 and the domain have no supports (free boundary conditions). (a) The result when optimized for minimum first eigenfrequency, (b) the result when optimized for maximum second eigenfrequency, (c) the result when maximizing the gap between first and second eigenfrequency.

$$B_e(t_e) = B_1 + t_e(B_2 - B_1) = (1 + t_e(\mu_B - 1))B_1, \tag{32}$$

where  $t_e$  is the element design parameter which, we recall, takes values between 0 and 1.

As an illustrative example we start with a domain where the ratio between the side lengths of the domain is 2/1 and the domain has free boundary conditions, i.e, we find the free–free modes.

In Fig. 7, the result of three different optimizations are shown: Fig. 7(a) shows the result when minimizing the first eigenfrequency, in Fig. 7(b) the maximization of the second eigenfrequency is shown, and finally in, Fig. 7(c) the result of maximizing the gap between the second and first eigenfrequencies is shown. It should be noted that by the notation of first and second eigenfrequencies we have neglected the rigid body mode.

In Figs. 7(a–c) the black color corresponds to material 2 and the white color corresponds to material 1. From Fig. 7 we see that the maximization of the gap between first and second eigenfrequencies clearly is a compromise between the results of minimizing first eigenfrequency and maximizing second eigenfrequency. It should be noted that for the case of maximizing the second eigenfrequency, this second eigenfrequency is a double eigenfrequency, and in the case of maximizing the gap between the two eigenfrequencies the second eigenfrequency is also a double eigenfrequency. In Fig. 7(a) we have a 0–1 design, i.e. no intermediate values of  $t_e$  are present, whereas in Figs. 7(b–c) there are some remaining elements with intermediate values, so-called “gray” elements.

To explain the gray elements we must discuss the interpolation (in some case penalization) that is used. For the optimizations shown in Fig. 7 the linear interpolation in Eqs. (31) and (32) are used. In Ref. [8] it was noted that the important aspect is not the interpolation of the stiffness (here coefficient  $A$ ) or the interpolation of the mass (here coefficient  $B$ ), but the interpolation of the eigenfrequency. The squared eigenfrequency  $\omega^2$  is by the Rayleigh quotient given as “stiffness divided by mass”. Using Eqs. (31) and (32), we find

$$\frac{A_e}{B_e} = \frac{(1 + t_e(\mu_A - 1)) A_1}{(1 + t_e(\mu_B - 1)) B_1} = f(t_e) \frac{A_1}{B_1}. \tag{33}$$

The curvature of Eq. (33) is such that intermediate values are penalized when an eigenfrequency is minimized. To achieve this intermediate values are penalized when an eigenfrequency is maximized, the curvature of the interpolation function,  $f(t_e)$  must have an opposite sign. This can be obtained in many ways and here it is chosen to let the interpolation be a second-order polynomial that goes through the three points

$$P_1 = (0, 1), \quad P_2 = (p_{2x}, p_{2y}), \quad P_3 = (1, \alpha).$$

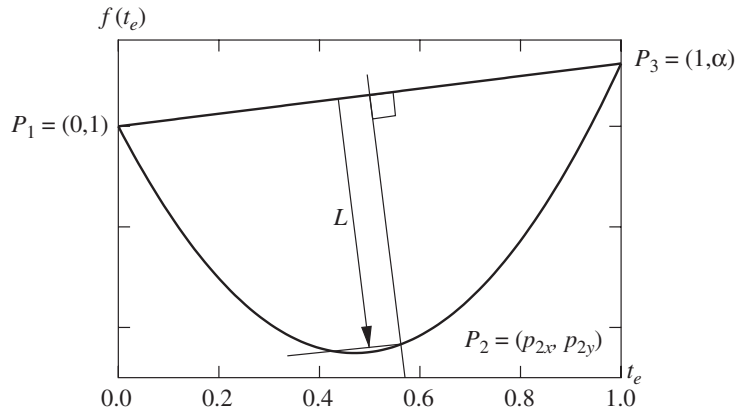


Fig. 8. Interpolation function of the squared eigenfrequency that simultaneously acts as a penalization function when eigenfrequencies are maximized.

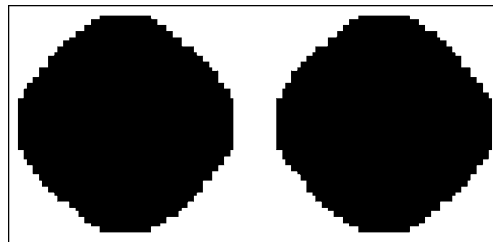


Fig. 9. Optimization of second eigenfrequency of a 2D domain with two different materials using interpolation (34), the ratio of the side lengths is 2/1 and the domain has no supports (free boundary conditions).

The three points are shown in Fig. 8. Point  $P_2$  is at a distance  $L$  along a line that is perpendicular to the linear interpolation and intersects this line at the center. The parameter  $L$  can be used in a continuation setting where the value of  $L$  is slowly increased during optimization to ensure 0–1 design. The penalization of  $A$  is then given by

$$A_e = f(t_e)B_e = (k_1(t_e)^2 + k_2t_e + 1) \cdot (1 + t_e(\mu_B - 1))A_1, \tag{34}$$

where  $k_1$  and  $k_2$  are constants that depend on the specific value of  $L$  and  $B_e$  is the linear interpolation (32), which seems reasonable from a physical point of view.

Using the new penalization function (34) together with Eq. (32) we achieve the optimized design in Fig. 9, where it is clear that the gray elements have been removed. However, there is still a problem with regard to the interpolation functions when the objective is to maximize the gap between two eigenfrequencies. The interpolation function shown in Fig. 8 with positive values of  $L$  is suited for the maximization of eigenfrequencies, whereas for negative values of  $L$  it is suited for the minimization. In the maximization of the gap we need both so we apply the following approach: when calculating the sensitivities of the constraints in Eq. (30) with respect to the lower bound  $C_2$  we calculate the eigenfrequencies and the sensitivities on the basis of the interpolation function (34) with  $L < 0$ . When we calculate the sensitivities of the constraints in Eq. (30) with

respect to the higher bound  $C_1$  we calculate the eigenfrequencies and the sensitivities on the basis of the interpolation function (34) with  $L > 0$ . The cost of using this method is that we have to calculate the eigenfrequencies twice.

### 3.4. Results for a square design domain

In the first examples we use material parameters corresponding to

$$\mu_A = 2.25, \quad \mu_B = 2.$$

First, we maximize the gap between eigenfrequencies for a square domain. A square design inherently has double eigenfrequencies even with only one material. If we want to maximize the gap between the first and second eigenfrequencies it is not possible to start from an initial design where all of the design values have been assigned a uniform value (e.g.  $t_e = 0.5$ ). To overcome this problem it is chosen to start from a design in which all design variables are assigned a finite value, e.g.  $t_e = 0.5$ , except for one element in which the value  $t_e = 0$  is used. With this small variation, there are no initial double eigenfrequency and the optimization works. We apply a continuation scheme in which the optimization is started with  $L = 0$  and the value of  $|L|$  is then increased during the optimization to ensure a final 0–1 design. This scheme also reduces the possibility of ending in a local minimum. Additionally, we always perform the optimization with different initial designs in order to ensure that we converge to the same minimum.

In Fig. 10, the results of optimizing the gap between eigenfrequencies are shown for  $n \in [1 : 12]$ . The design domain is discretized in  $100 \times 100$  elements. As it appears from the figure, the new penalization scheme has enabled us to obtain optimized structures with a well-defined distribution of the two materials. Only very few gray elements appear such as those near the corners for  $n = 7$  and  $n = 12$ . For some modes it appears that the pattern observed in 1D is valid here as well, i.e. the optimal design is periodic like with the periodicity increasing with increasing mode order. For other modes ( $n = 5, n = 10, n = 11$  and  $n = 12$ ) the optimized design show a different topological distribution of the two materials.

### 3.5. Results for a rectangular design domain

In the next examples the same method of optimization has been used but in this case the design domain size is changed so that the ratio of the side length is 2/1. The results of the optimizations are shown in Fig. 11. The design domain is here discretized in  $100 \times 50$  elements.

The results depicted in Fig. 11 are similar to the results for the square domain with some topologies being periodic like and others being qualitatively different. We now try to examine if the general results from 1D can be transferred to the 2D case.

### 3.6. Maximizing the ratio of adjacent eigenfrequencies

As in the 1D case we now change the objective function to that in Eq. (13) so that the ratio between adjacent eigenfrequencies is maximized, but we still use the double-bound formulation introduced in Eq. (30). We repeat the optimization for the rectangular domain for the case where  $n = 7$ , i.e. corresponding to the design in Fig. 11(g).



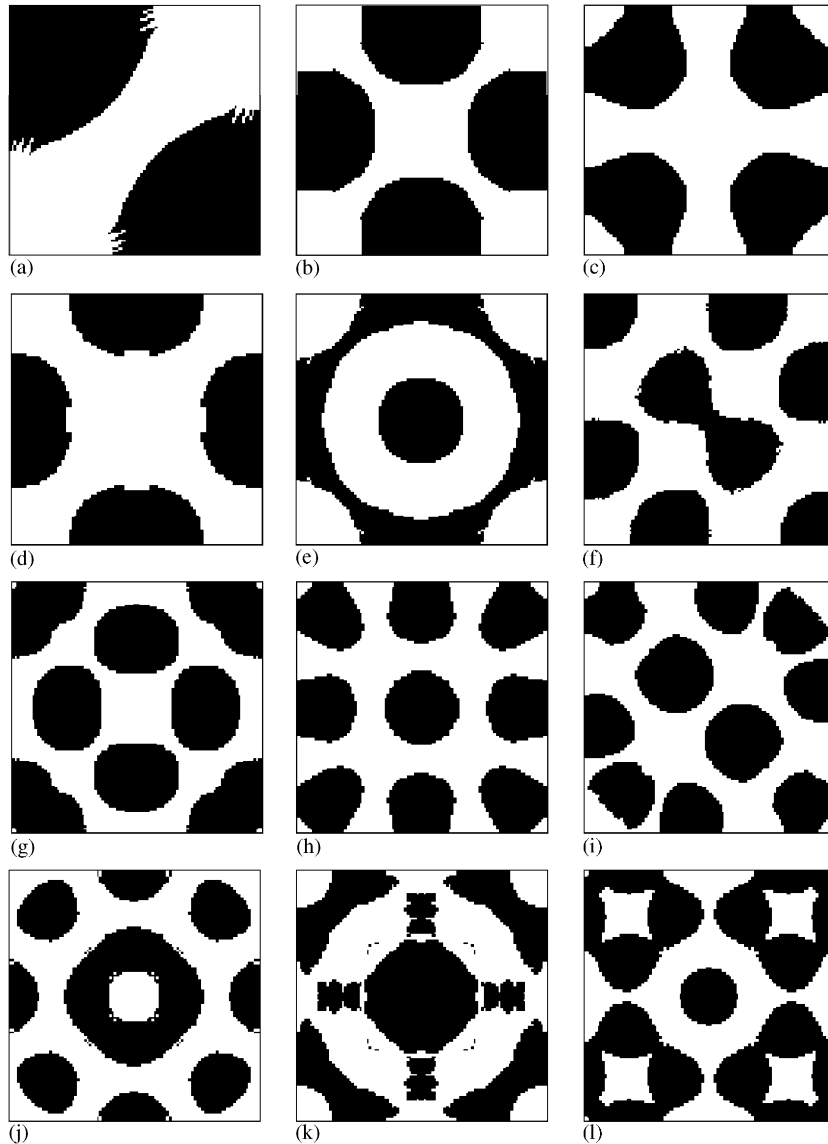


Fig. 10. Eigenfrequency optimization of a 2D domain with two different materials, the design domain is a square that has no supports (free boundary conditions). (a) The result when maximizing the gap between 1st and 2nd eigenfrequency ( $n = 1$ ), (b)  $n = 2$ , (c)  $n = 3$ , (d)  $n = 4$ , (e)  $n = 5$ , (f)  $n = 6$ , (g)  $n = 7$ , (h)  $n = 8$ , (i)  $n = 9$ , (j)  $n = 10$ , (k)  $n = 11$ , (l)  $n = 12$ .

We change the values  $\mu_A$  and  $\mu_B$  so that the value of  $\alpha$  is changed but the value of  $\beta = 4.5$  is kept fixed. The results are shown in Fig. 12(a–c). The value of the objective, i.e. the ratio between the squared eigenfrequencies, does not vary significantly but is not exactly constant as in the 1D case. The value of  $\omega_8^2/\omega_7^2$  is 2.12, 2.06 and 2.00 for Figs. 12(a–c), respectively.

When we compare Figs. 12(a–c) it is clear that although the value of the objective stays almost constant the design change is evident. In the final examples we fix the value of  $\alpha = 1.125$  and

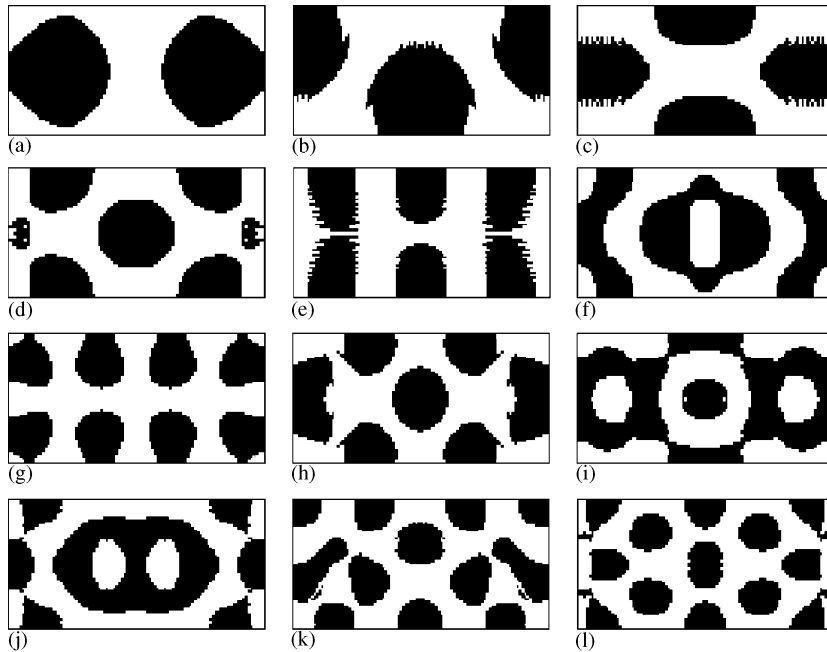


Fig. 11. Eigenfrequency optimization of a 2D domain with two different materials, the ratio of the side length is 2/1 and the domain has no supports (free boundary conditions). (a)  $n = 1$ , (b)  $n = 2$ , (c)  $n = 3$ , (d)  $n = 4$ , (e)  $n = 5$ , (f)  $n = 6$ , (g)  $n = 7$ , (h)  $n = 8$ , (i)  $n = 9$ , (j)  $n = 10$ , (k)  $n = 11$ , (l)  $n = 12$ .



Fig. 12. Maximizing the separation of 7th and 8th eigenfrequencies ( $n = 7$ ). Compared to Fig. 11 the objective is here the ratio between the squared eigenfrequencies and the value of  $\alpha$  is changed but the value of  $\beta = 4.5$  is kept fixed. (a)  $\alpha = 2$ ,  $\omega_8^2/\omega_7^2 = 2.12$ , (b)  $\alpha = 4$ ,  $\omega_8^2/\omega_7^2 = 2.06$ , (c)  $\alpha = 8$ ,  $\omega_8^2/\omega_7^2 = 2.00$ .

instead vary the value of  $\beta$ . The results of the optimization are shown in Fig. 13(a–c) and the objective values are 2.99, 4.18 and 5.89, respectively. The figures show that we achieve the opposite result compared to when the value of  $\alpha$  is changed; the objective value is changed considerably but the design stays more or less the same.

#### 4. Conclusions

In this paper, we consider optimal design of 1D and 2D structures for which the vibrations are governed by the scalar wave equation. The method of topology optimization is used to maximize

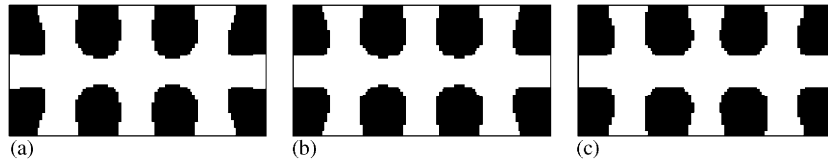


Fig. 13. Maximizing the separation of 7th and 8th eigenfrequencies ( $n = 7$ ). Compared to Fig. 11 the objective is here the ratio between the squared eigenfrequencies and the value of  $\beta$  is changed but the value of  $\alpha = 1.125$  is kept fixed. (a)  $\beta = 9$ ,  $\omega_8^2/\omega_7^2 = 2.99$ , (b)  $\beta = 18$ ,  $\omega_8^2/\omega_7^2 = 4.18$ , (c)  $\beta = 36$ ,  $\omega_8^2/\omega_7^2 = 5.89$ .

the separation of two adjacent eigenfrequencies for structures with two different material components.

The optimization procedure is based on finite element analysis with a single continuous design variable assigned to each element. This design variable  $t_e$  is defined so that for  $t_e = 0$  the material properties in that element are those of material 1 and for  $t_e = 1$  the properties correspond to material 2. For intermediate values of  $t_e$  the material properties are also intermediate and a special interpolation formulation is introduced in the 2D case to ensure that only the two materials appear in the final optimized design. In the 2D case we treat multiple eigenfrequencies both in relation to the sensitivity calculations but also by reformulating the objective into a double-bound formulation.

Two different formulations are used for maximizing the separation of the eigenfrequencies. The first approach is to use the maximum difference in the frequencies as the optimization objective. For both the 1D and the 2D cases the optimized designs are well-defined 0–1 designs, i.e. no intermediate materials appear in the optimal designs. In 1D the optimized structures are periodic-like and there is a direct relation between the mode order and the number of alternating sections of materials 1 and 2. In the 2D case, square and rectangular domains are studied, and it is seen that the optimized designs for some modes consist of periodically placed inclusions as in 1D, whereas for other modes a quite different topology is obtained.

In the second optimization formulation we maximize the ratio of two adjacent eigenfrequencies. Two material parameters are introduced:  $\alpha$  and  $\beta$  that are functions of the material coefficients of the two materials. In 1D it is shown that the material distribution in the final optimized design appears to depend only on  $\alpha$ , whereas the maximum ratio for this design depends only on  $\beta$ . For 2D a similar relation appears, but unlike in 1D an exact correspondence is not seen. Additionally, it is seen that in 1D the maximum ratio that can be obtained between adjacent eigenfrequencies seems to be independent of the mode order  $n$  for high values of  $n$ . This phenomenon was not studied in 2D.

## Acknowledgements

The work of Jakob S. Jensen was supported by the Danish Technical Research Council through the project “Designing bandgap materials and structures with optimized dynamic properties”.

## References

- [1] M.P. Bendsøe, N. Kikuchi, Generating optimal topologies in structural design using a homogenization method, *Computer Methods in Applied Mechanics and Engineering* 71 (2) (1988) 197–224.
- [2] M.P. Bendsøe, O. Sigmund, *Topology Optimization—Theory, Methods and Applications*, Springer, Berlin, Heidelberg, 2003.
- [3] A. Diaz, N. Kikuchi, Solution to shape and topology eigenvalue optimization problems using a homogenization method, *International Journal for Numerical Methods in Engineering* 35 (1992) 1487–1502.
- [4] C.A. Soto, A.R. Diaz, Layout of plate structures for improved dynamic response using a homogenization method, *Advances in Design Automation* 1 (1993) 667–674.
- [5] Z.-D. Ma, H.-C. Cheng, N. Kikuchi, Structural design for obtaining desired eigenfrequencies by using the topology and shape optimization method, *Computing Systems in Engineering* 5 (1) (1994) 77–89.
- [6] M.P. Bendsøe, O. Sigmund, Material interpolations in topology optimization, *Archive of Applied Mechanics* 69 (1999) 635–654.
- [7] I. Kosaka, C.C. Swan, A symmetry reduction method for continuum structural topology optimization, *Computers and Structures* 70 (1999) 47–61.
- [8] N.L. Pedersen, Maximization of eigenvalues using topology optimization, *Structural and Multidisciplinary Optimization* 20 (2000) 2–11.
- [9] N.L. Pedersen, On topology optimization of plates with pre-stress, *International Journal of Numerical Methods in Engineering* 51 (2) (2001) 225–239.
- [10] M.M. Sigalas, E.N. Economou, Elastic and acoustic wave band structure, *Journal of Sound and Vibration* 158 (2) (1992) 377–382.
- [11] J.S. Jensen, Phononic band gaps and vibrations in one- and two-dimensional mass-spring structures, *Journal of Sound and Vibration* 266 (5) (2003) 1053–1078.
- [12] S.J. Cox, D.C. Dobson, Maximizing band gaps in two-dimensional photonic crystals, *SIAM Journal for Applied Mathematics* 59 (6) (1999) 2108–2120.
- [13] S.J. Cox, D.C. Dobson, Band structure optimization of two-dimensional photonic crystals in *h*-polarization, *Journal of Computational Physics* 158 (2) (2000) 214–224.
- [14] O. Sigmund, Microstructural design of elastic band gap structures, in: G.D. Cheng, Y. Gu, S. Liu, Y. Wang (Eds.), *Proceedings of the Fourth World Congress of Structural and Multidisciplinary Optimization WCSMO-4*, Dalian, China, 2001, CD-rom.
- [15] O. Sigmund, J.S. Jensen, Systematic design of phononic band-gap materials and structures by topology optimization, *Philosophical Transactions of the Royal Society London, Series A (Mathematical, Physical and Engineering Sciences)* 361 (2003) 1001–1019.
- [16] Z.-D. Ma, N. Kikuchi, I. Hagiwara, Structural topology and shape optimization for a frequency response problem, *Computational Mechanics* 13 (1993) 157–174.
- [17] C.S. Jog, Topology design of structures subjected to periodic loading, *Journal of Sound and Vibration* 253 (3) (2002) 687–709.
- [18] S. Osher, F. Santosa, Level set methods for optimization problems involving geometry and constraints i. frequencies of a two-density inhomogeneous drum, *Journal of Computational Physics* 171 (2001) 272–288.
- [19] K. Svanberg, The method of moving asymptotes—a new method for structural optimization, *International Journal for Numerical Methods in Engineering* 24 (1987) 359–373.
- [20] K.J. Bathe, *Finite Element Procedures*, second ed., Prentice-Hall, Englewood Cliffs, NJ, 1996.
- [21] A.P. Seyranian, E. Lund, N. Olhoff, Multiple eigenvalues in structural optimization problems, *Structural Optimization* 8 (4) (1994) 207–227.
- [22] N.L. Pedersen, A.K. Nielsen, Optimization of practical trusses with constraints on eigenfrequencies, displacements, stresses and buckling, *Structural and Multidisciplinary Optimization* 25 (2003) 436–445.